

# Numerical Study of the Fluid Flow in a Passive Tangential Vortex Tube



Simeon Livshits, Natalia Yudina, Ruslan Lebedev, Svetlana Enikeeva, and Evgeny Panamarenka

## 1 Introduction

Recently, there has been a clear trend towards the decentralization of heat supply networks. This process has covered almost all the technically developed countries of Europe and America, and every year it is becoming more and more noticeable in Russia. Thus, in recent years, the commissioning of boiler houses with a capacity of 100 Gcal/hour and above has been practically stopped, and autonomous heat supply systems are increasingly preferred. In addition to the existing and actively developing classical directions of autonomous heat supply systems, in the 90 s of the twentieth century, a promising direction of individual heat supply based on the use of vortex heat generators received a new round of development.

Currently, heat generators are used for heating and hot water supply to consumers (including as emergency or autonomous sources) in places where there are no centralized heat supply systems. Unlike traditional central heating systems, which are characterized by high material consumption and require significant space for equipment placement, fuel supply and the cost of transporting the final product to the consumer, autonomous systems designed on the basis of vortex heat generators do not require fuel storage and transportation costs, reduce heat loss to a minimum, are simple in design and do not require significant maintenance costs.

---

S. Livshits (✉) · N. Yudina  
Kazan State Power Engineering University, Krasnoselskayast., 51, Kazan 420066, Russia

R. Lebedev  
Gazprom VNIIGAZ LLC, Moscow, Russia

S. Enikeeva  
Kazan National Research Technological University, Kazan, Russia

E. Panamarenka  
Belarusian National Technical University, Independence Avenue 65, Minsk, Belarus

Since the appearance of the first static-acting vortex apparatuses, there has been an active debate about the nature of the occurrence of the effect, which has been defined in the literature as “mechanical activation” of the working flow [1–3].

Unfortunately, at the moment there is no proper scientific justification for the observed effect of “mechanical activation”. In this regard, there is an important task of detailed study of the physical and chemical nature of the interaction realized in heat generators of the cavitation-vortex type.

## 2 Literature Review

The analysis of works devoted to this problem allows us to distinguish two of the most frequently encountered opinions that characterize the physics of the process:

1. the presence of structural changes in the working fluid flow at the intermolecular level (due to the formation of hydrogen bonds between the liquid molecules, the process of forming associates occurs, accompanied by a change in temperature) [1];
2. When the liquid moves, energy is released due to the collapse of cavitation bubbles, which results in an increase in the flow temperature [2].

Proponents of the second hypothesis point out that the thermo kinetic process under consideration takes place in a state far from equilibrium. The energy supply in the nonequilibrium state is associated with the processes characteristic of dissipative structures [2].

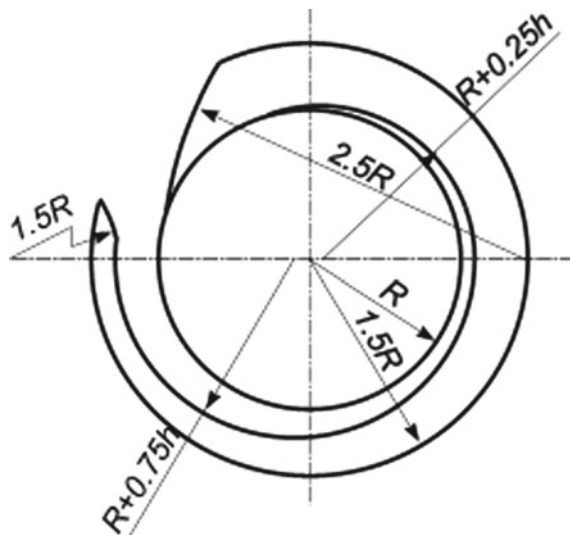
Cavitation—as a phenomenon has become the subject of numerous studies during the period when scientists were faced with such a complex and potentially dangerous phenomenon as the longitudinal oscillatory instability observed in high-flow fuel supply systems of launch vehicles, in turbine engines of civil and military aircraft [4, 5].

In vortex heat generators, cavitation, on the contrary, brings a positive effect, consisting in an increase in temperature [2], this indicates the need for its in-depth study. The complexity of the hydrodynamic conditions of the working flow can affect the distribution of the local areas of cavitation origin, so the numerical experiment allows not only to study in detail the processes accompanying cavitation, but also to identify the areas of its occurrence to find the optimal geometric parameters of the installation [6].

## 3 Materials and Methods

To date, the most rational and affordable method of studying physical processes is numerical modeling, implemented in specialized software packages. The choice of

**Fig. 1** The scheme of the nozzle device according to Merkulov



this method is supported by the convenience of processing, analyzing, and presenting data (i.e., visualization) using computer graphics.

Modeling of three-dimensional fluid flow in a passive tangential vortex heat generator was carried out using the Flow Vision software package, based on the finite-volume method for solving hydrodynamic equations [6].

The first stage of the simulation was the creation of a computational domain for the constructed mathematical model.

As a reference model, a vortex tube with a nozzle inlet developed by A. P. Merkulov was adopted (Fig. 1).

This model combines high efficiency, simplicity, and low cost of manufacturing. However, despite all its advantages over the others, with a single fluid flow input, the vortex axis does not coincide with the axis of the working chamber in the nozzle section, which negatively affects the process of forming an axisymmetric vortex flow and the hydrodynamics of the vortex flow in the working chamber. An increase in the number of inputs should be accompanied by a decrease in the intensity of disturbances exerted on the swirling space of the water flow in the working chamber. The study and analysis of the most well-known high-precision twisting systems have shown that the centrifugal nozzle with four nozzle inputs has the lowest losses and the best effect of twisting the flow (Fig. 2).

In a centrifugal nozzle, a coolant is fed through tangential channels to the working chamber of the swirling device. The flow in it is twisted and is supplied to the nozzle. At the nozzle section, under the influence of internal hydro-mechanical forces, the membrane is crushed into small droplet-like fractions and enters the working area at a certain opening angle. Due to the centrifugal force, the flow is pressed against the walls and a region of reduced pressure is formed around the axis. When exiting the jet-twisting device, in order to avoid flow disruption, it is necessary to minimize

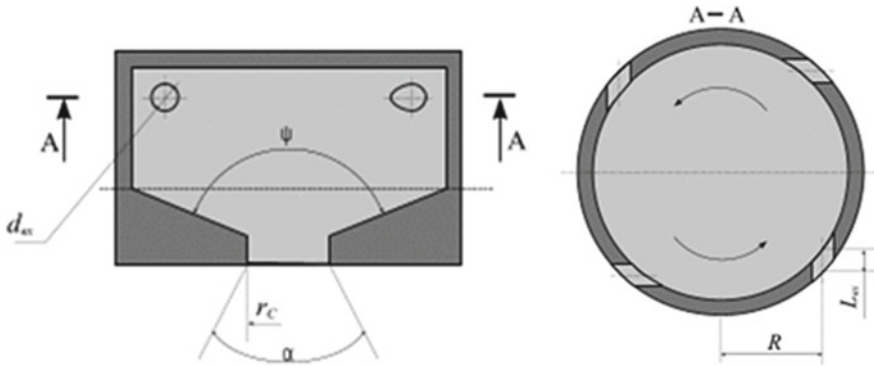


**Fig. 2** Diagram of the centrifugal nozzle ( $R$ —twist shoulder;  $d_v, L_v$ —the diameter and length of the tangential channels;  $\psi$ —angle of the cone part;  $\alpha$ —the angle of the stream output)

the length of the nozzle, and the diameter of the nozzle outlet should be as large as possible for each specific mode. Tangential channels can be circular or rectangular in cross-section.

Adapting the theory of the centrifugal nozzle [4] to the problem of designing the nozzle inlet of a passive tangential vortex heat generator, and taking the initial parameters of the water flow: the pressure before entering the nozzle channels  $p = 0.7 \cdot 10^6$  Pa; initial temperature before entering the nozzle channels  $t = 20$  °C; mass flow through the swirling device  $G = 4005.2$  kg/h, According to the calculated data in the COMPASS 3D CAD, the three-dimensional space of the working flow was modeled for models with a nozzle input of the nozzle type (Fig. 3) and with a Merkulov nozzle inlet (Fig. 4).

The calculated area is the volume of the internal space of the vortex heat generator (see Figs. 3 and 4). The surface of the calculated area is a collection of flat polygons-facets. In the study of hydrodynamic characteristics, the interaction of flows in the

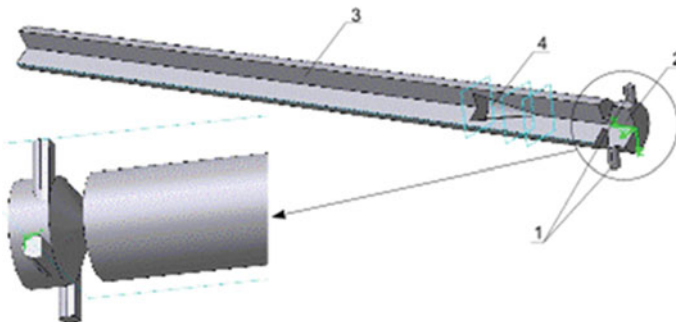


**Fig. 3** A three-dimensional solid-state model with a flow input calculated by the author in the first modification; 1—tangential flow inputs; 2—a jet-twisting device; 3—a rectilinear cylindrical working chamber; 4—a brake cone-shaped device

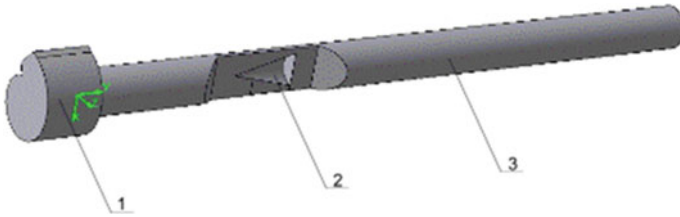


**Fig. 4** Three-dimensional solid-state model of the internal space of a passive tangential vortex heat generator with a nozzle input by A. P. Merkulov. 1—Nozzle inlet according to A. P. Merkulov; 2—brake cone-shaped device; 3—straight cylindrical working chamber

area of the brake device location and at the exit from the swirling device is of particular interest.

The study of the influence of the geometry of the working area of the heat generator on the thermal efficiency of its operation was carried out with the same linear characteristics of the working chamber and the vortex twisting device [7, 8]. Only the area of the brake device location was changed at the initial section of the working chamber ( $L = 200$  mm), in its middle part ( $L = 400$  mm) and at the end of the working chamber ( $L = 600$  mm) with the calculated length of the working space  $L = 800$  mm.

The purpose of the calculation was to simulate the fluid motion in the calculated region to obtain the pressure and temperature field distributions at any point in the internal space of the vortex heat generator.

As a mathematical model for describing the motion, the “weakly compressible fluid” model was chosen, which allows us to model the flow at large Reynolds numbers and modes in which cavitation is possible [8]. For the numerical solution of the equations of the standard mathematical the turbulence model  $\kappa - \varepsilon$  adopted a rectangular adapted locally ground grid.

The “weakly compressible fluid” model describes the motion of a viscous fluid at subsonic Mach numbers and various density changes, using the method of joint solution of the equations of motion, energy, and  $\kappa - \varepsilon$  turbulence.

As the boundary conditions for the solution of the problem under consideration, the following are chosen:

the normal flow rate at the entrance to the channel model:

$$V|_0 = V|_n \tag{1}$$

$$P|_0 = \text{const} \tag{2}$$

the logarithmic law for the velocity profile in a turbulent boundary layer:

$$V \approx \sqrt{\frac{\sigma}{\rho}} \ln \frac{x}{C} \tag{3}$$

where  $C, \sigma$ —is the integration constants,  $\rho$ —flow density,  $x$ —the current coordinate;  
The model is represented by the Eqs. (4), (6), (9) and (10).

Navier–Stokes equations

$$\frac{\partial \rho V}{\partial t} + \nabla(\rho V \otimes V) = -\nabla P + \nabla((\mu + \mu_t)(\nabla V + (\nabla V)^T)) + S \quad (4)$$

where  $V$  is the velocity;  $t$  is the temperature;  $P$  is the pressure;  $\mu, \mu_t$  are the dynamic and turbulent viscosity;  $S$  is the dimensionless parameter characterizing the source.

The energy equation

$$\frac{\partial(\rho h)}{\partial t} + \nabla(\rho V h) = \nabla\left(\left(\frac{\lambda}{C_p} + \frac{\mu_t}{Pr_t}\right)\nabla h\right) + Q \quad (5)$$

where  $h$  is the enthalpy,  $\lambda$  is the coefficient of thermal conductivity,  $C_p$  is the specific heat capacity,  $Q$  is the heat source, and  $Pr_t$  is the turbulent Prandtl number [11].

To determine the concentration of bubbles in the flow, the convective-diffusion transport equation is solved:

To determine the concentration of bubbles in the flow, the convective-diffusion transport equation is solved:

$$\frac{\partial(\rho C)}{\partial t} + \nabla(\rho V C) = \nabla\left(\left(\frac{\mu}{Sc} + \frac{\mu_t}{Sc_t}\right)\nabla C\right) \quad (6)$$

$Sc_t$ —the turbulent Schmidt number.

In the accepted standard  $k$ - $\varepsilon$  turbulence model, the turbulent viscosity  $\mu_t$  is expressed in terms of the values  $k$  and  $\varepsilon$  as follows:

$$\mu_t = C_p \rho \frac{k^2}{\varepsilon} f_\mu \quad (7)$$

where  $k$  is the turbulent energy,  $\varepsilon$  is the rate of dissipation of the turbulent energy,  $f_\mu = f_1 = 1$ .

The equations for  $k$  and  $\varepsilon$  have the form:

$$\frac{\partial(\rho k)}{\partial t} + \nabla(\rho V k) = \nabla\left(\left(\mu + \frac{\mu_t}{\sigma_k}\right)\nabla k\right) + \mu_t G - \rho \varepsilon \quad (8)$$

$$\frac{\partial(\rho \varepsilon)}{\partial t} + \nabla(\rho V \varepsilon) = \nabla\left(\left(\mu + \frac{\mu_t}{\sigma_\varepsilon}\right)\nabla \varepsilon\right) + C_1 \frac{\varepsilon}{k} \mu_t G - C_2 f_1 \rho \frac{\varepsilon^2}{k} \quad (9)$$

where  $\sigma_k = 1, \sigma_\varepsilon = 1.3, C_1 = 1.44, C_2 = 1.92$ —standard model constants  $k$ - $\varepsilon$  turbulence.

$$G = D_{ij} \frac{\partial V_i}{\partial x_j} \tag{10}$$

$$D_{ij} = S_{ij} - \frac{2}{3} \left( \nabla \cdot V + \frac{\rho k}{\mu_t} \right) \delta_{ij} \tag{11}$$

$$S_{ij} = \frac{\partial V_i}{\partial x_j} + \frac{\partial V_j}{\partial x_i} \tag{12}$$

$D$ —the doubled strain rate tensor.

## 4 Results

Figure 5 presents the results of a numerical experiment of the flow of a weakly compressible fluid for a passive tangential vortex heat generator with a nozzle input by A. P. Merkulov and with the flow input proposed in this article [12].

After entering the flow through the tangential channels into the working chamber [15] (Fig. 5a), there is a slight decrease in pressure, which may be a consequence of pressure losses, both in the tangential channels themselves, and as a result of the interaction of flows in the working chamber of the jet-twisting device [16]. After the flow enters the working chamber of the heat generator (due to the specific geometry of the channel and the complexity of the movement), there is a sharp drop in the flow pressure to the level of the saturation temperature, and it is in this region that the liquid–vapor phase transition occurs. Further movement of the flow is accompanied by an increase in pressure, which is caused by the presence of a braking device. As a result, the resulting vapor bubbles collapse [17]. The region from the input of the flow into the working chamber to the braking device, based on the theory set out in [2], should be called the cavitation region. The further pressure drop is obviously due to the process of re-forming the flow after the brake device and the presence of roughness.

As can be seen from the graph (Fig. 5a, b), cavitation is possible only when the brake device is located at a distance of  $L = 200$  mm from the end wall of the swirl chamber. In the other two cases, when  $L = 400$  and  $L = 600$  mm, the pressure drop to the saturation state did not occur. The location of the brake device affects the flow characteristics in the area from the nozzle to the area of the brake device [18].

In the graph (Fig. 5b), after the flow enters through the Merkulov nozzle inlet in the swirling chamber, there is a slight decrease in pressure due to losses associated with both the interaction of the flows and the change in the velocity vector, and with hydraulic losses [19]. The further increase is due to the action of mass forces caused by the movement around the circle [20].

Figure 5b and d, shows a graph of visualization of the calculation data in each cell by temperature, for three variants of the location of the braking devices.

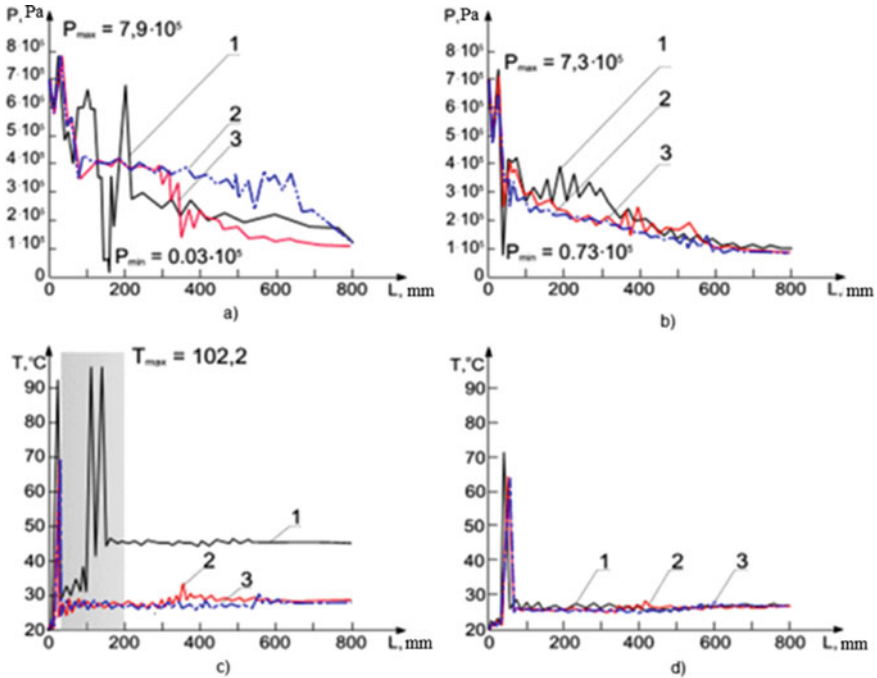


**Fig. 5** The results of numerical experiment on the argument the total pressure (a) and (b), the argument of the temperature field (c) and (d): a, c with jet-twisting device type—“atomizer”, b, d with jet-twisting device according to the type of snail (A. P. Merkulov) [13]. 1—working flow pressure line for a model of a vortex generator with a braking device removed at a distance of 200 mm from the end wall of the swirling chamber; 2—working flow pressure line for a model of a vortex generator with a braking device removed at a distance of 400 mm from the end wall of the swirling chamber; 3—working flow pressure line for a model of a vortex generator with a braking device removed at a distance of 600 mm from the end wall of the swirling chamber [14]

In Fig. 5b, curve 1 has three maxima at the interval from 0 to 170 mm. Also, in the range from 0 to 170 mm, a minimum is observed at a temperature of 20 °C and a pressure of 3.5 kPa, which characterizes the evaporation process, as a result of which the flow temperature decreases on average by 3 ÷ 4 °C. The size of the area of possible cavitation has a huge impact on the percentage of the liquid being boiled. Therefore, the main task is to artificially increase the area of cavitation origin. Obviously, the further a braking device is located from the nozzle part of the swirler, the less effective halogenerator. This is due to the presence of reverse flow, which has a strong effect on the outgoing flow of the twisting device, leading to a decrease in heat generation [9]. The gradual increase in temperature behind the braking device is due to a decrease in turbulence pulsations and flow velocity in general, as a result of which the only source of heat—the dissipation of internal energy, due to a constant decrease in tangential stresses that directly depend on the main flow parameters, tends to zero, which is well illustrated by the graph in (Fig. 5b and d).



The nature of the temperature function in (Fig. 5d) is similar to the graph shown in (Fig. 5c), but there is no clearly defined cavitation region. The flow temperature increases by  $5^{\circ} - 8^{\circ} \text{C}$ , which indicates a low efficiency of the input type “A. P. Merkulov”, and the temperature increase is explained by the presence of viscous friction forces.

## 5 Conclusions

As a result of the numerical experiment for the proposed jet-twisting device, the distributions of velocities, pressure, heat flow, and liquid temperature at all points of the calculated space were obtained, which made it possible to evaluate the efficiency of the design of the alternative jet-twisting device and the vortex tube as a whole. The flow temperature increased by an average of  $25^{\circ} \text{C}$ .

## References

1. Merkulov, A.: Vortex effect and its application in engineering. *Mashinostroenie* (1969)
2. Suslov, A., Ivanov, S., Murashkin, A., Chizhikov, Y.: Vortical apparatuses. *Mashinostroenie* (1985)
3. Merkulov, A.: Vortical effect and its application in engineering. *Kuibyshev, KuAI* (1988)
4. Adamov, V.: Burning of fuel oil in boiler furnaces (1989)
5. Serebryakov, R.: Heat generator with vortex cavitation of the working body. *Bulletin of Agrarian Science Don* 4 (2016)
6. Akhmetov, Y., Kalimullin, R., Tselishchev, V.: Numerical and physical modeling of a liquid flow in a vortex heat generator. *Bull. Ufa State Aviation Tech. Univ.* **4**, 39 (2010)
7. Piralishvili, S.: Vortex effect. Theory, experiment, numerical simulation. In: *Collection of Scientific Papers SWorld*, vol. 3, 3 (2013)
8. Gorbenko, V.: Numerical simulation of temperature fields of complex-shaped bodies on the principle of diaktotics. *Bull. South Ural State University, Series: Energy* **20**, 92 (2007)
9. Iokova, I., Tarasevich, E.: Study of the possibility of application of a vortex heat generator in the heat supply systems of residential, industrial and public buildings. *Energy: News Higher Educ. Inst. Energy Assoc. CIS* **61**, 2 (2018)
10. Dutta, T., Sinhamahapatra, K.P., Bandyopadhyay, S.S.: Experimental and numerical investigation of energy separation in counterflow and uniflow vortex tubes | [Étude expérimentale et numérique de la séparation de l'énergie dans les tubes vortex à contre-courant et à courant parallèle]. *International Journal of Refrigeration* 123 (2021)
11. Wang, K., Xie, L., Ouyang, X., Wang, H., Han, T., et al.: Numerical simulation on the flow and temperature field of natural gas single circuit vortex tubes. *Natural Gas Industry* **40**(7) (2020)
12. Lagrandeur, J., Poncet, S., Sorin, M.: Review of predictive models for the design of counterflow vortex tubes working with perfect gas. *Int. J. Therm. Sci.* **142** (2019)
13. Rehman, A., Athar, M., Mansoor, T.: Mechanism of vortex motion. *ISH J. Hydraul. Eng.* **23**(2) (2017)
14. Novikova, O.V., Erastov, A.E., Livshits, S.A.: Features of evaluating the efficiency indicators of the electric power enterprise. In: *E3S Web of Conferences*, vol. 124 (2019)
15. He, L.-J., Wang, S.-X., Wu, X.-W., Sun, S.-Z.: Effect of nozzle structure on the performance of vortex tube. *Reneng Dongli Gongcheng/J. Eng. Therm. Energy Power* **35**(6) (2020)

16. You, Y., Seibold, F., Wang, S., Weigand, B., Gross, U.: URANS of turbulent flow and heat transfer in divergent swirl tubes using the  $k$ - $\omega$  SST turbulence model with curvature correction. *Int. J. Heat Mass Transfer* **159** (2020)
17. Pan, H., Pan, P.: Effect of hot-end tube diameter on flow field of vortex tube: a simulation study. **40**(7) (2020)
18. Wang, J., He, X., Li, J., Zou, S., Xu, H., et al.: Simulation of heat transfer enhancement and flow resistance characteristics of twisted slice tubes with openings. *Guocheng Gongcheng Xuebao/The Chinese J. Process Eng.* **20**(5) (2020)
19. Li, R., Hu, Z., Gao, Y.: Numerical simulation of energy separation in a vortex tube with different vane number rectifiers. In: *Proceedings of the 31st Chinese Control and Decision Conference, CCDC* (2019)
20. Shamsoddini, R., Abolpour, B.: A geometric model for a vortex tube based on numerical analysis to reduce the effect of nozzle number. *Int. J. Refrig.* **94** (2018)